Assessment of Uncertainties in Aquarius Salinity Retrievals

Algorithm Theoretical Basis Document

Thomas Meissner

Remote Sensing Systems, Santa Rosa, CA

Prepared for

Aquarius Data Processing System

Aquarius Science and Cal/Val Teams

Remote Sensing Systems
444 Tenth Street, Suite 200, Santa Rosa, CA 95401 (707) 545-2904

Assessment of Uncertainties in Aquarius Salinity Retrievals

Thomas Meissner

Remote Sensing Systems

Version 2: 06/10/2015

ABSTRACT

This memo presents a method for formally assessing random and systematic uncertainties in the Aquarius salinity retrievals. The method is based on performing multiple retrievals by perturbing the various inputs to the retrieval algorithm and calculating the sensitivity of the Aquarius salinity to these inputs. Together with an error model for the uncertainties in the input parameters it is possible to calculate the uncertainty in the retrieved SSS. It is important to distinguish between random uncertainties, which get suppressed when computing weekly or monthly averages and systematic uncertainties, which do not get suppressed by taking averages. We have compared the results of the formal uncertainty estimates with uncertainty estimates based on comparing the Aquarius salinities with those from external validation sources finding very good agreement.

1. FORMAL ASSESSMENT OF UNCERTAINTIES

The basic approach to formally assess an uncertainty of the Aquarius salinity retrieval $S(x_i,\ldots)$ to a parameter x_i is to calculate the sensitivity of S to x_i. This is done by running the standard Aquarius Level 2 algorithm and perturbing its input x_{i0} by a small perturbation $\pm\Delta x_i$. The sensitivity is then computed as the derivative:

$$\frac{\partial S}{\partial x_i}(x_{i0}) \approx \frac{S(x_{i0}+\Delta x_i) - S(x_{i0}-\Delta x_i)}{2\cdot\Delta x_i} \tag{1}$$

Assuming that we have an uncertainty estimate $\Delta x_i(x_{i0})$ for the parameter x_i, then the corresponding uncertainty in S is given by:

$$\Delta S_i(x_{i0}) \approx \frac{\partial S}{\partial x_i}\cdot\Delta x_i \tag{2}$$

The assessment of the uncertainty in S consists in two parts:

1. The computational/algorithm part: Running the retrieval algorithm with the perturbed parameter values.
2. Obtaining a realistic error model for all the uncertainties that are involved. This part is done offline and its results are fed into the perturbed retrievals.

Performing the uncertainty estimation this way takes into account that a given uncertainty in one of the input parameter can translate to very different uncertainties in the retrieved salinity depending on the environmental scene. For example the same error in the input wind speed that is used in the surface roughness correction or in the reflected galactic radiation will result in a much larger uncertainty in salinity in cold water where the sensitivity of the T_B to salinity is low than it would in warm water where the sensitivity is higher. The SST of the scene is a major driver in the size of the salinity uncertainty.

2. PROPAGATION OF UNCERTAINTIES

2.1 Random and Systematic Uncertainties

We need to assign uncertainties to both the Level 2 (L2) and to the Level 3 (L3) Aquarius salinity products. The propagation of the uncertainties from the 1.44 sec measurement (L2) to the L3 averages is not straightforward, as the uncertainties have both random and systematic components. Whereas the random components are getting suppressed by a factor $1/\sqrt{N}$ when averaging over N samples, the systematic components do not but the uncertainty of the average remains simply the average of the individual uncertainties. As a consequence, it is necessary to separately assess a random uncertainty Δx_i^{ran} and a systematic uncertainty Δx_i^{sys} for each parameter x_i. This separation is also not straightforward and not unambiguous. As a general guideline:

1. Uncertainties that fluctuate on larger time and spatial scales (1 month, > 100 km) are treated as systematic uncertainties.
2. Uncertainties that fluctuate on shorter time and spatial scales are treated as random uncertainties.

Every L2 salinity retrieval and every L3 map cell will contain two uncertainty values: a random uncertainty and a systematic uncertainty . The total RMS uncertainty is defined by:

$$\Delta S = \sqrt{\left(\Delta S^{sys}\right)^2 + \left(\Delta S^{ran}\right)^2} \tag{3}$$

In the following we address the error propagation of both random and systematic uncertainties for the L2 retrievals and the creating the L3 maps.

2.2 Uncertainty Propagation within the L2 Algorithm

The retrieved salinity $S\left(x_i\right)$ depends on a number of parameters $x_i, i = 1,\ldots M$, which all have separate uncertainties $\Delta x_i, i = 1,\ldots M$. The error model will assume that all of these uncertainties are mutually independent. However, the retrieval algorithm and the geophysical model function can introduce correlations between the different horns and polarizations. For example, radiometer noise is uncorrelated in all channels, whereas an uncertainty in SST results in certain correlations among the different channels.

1) Random uncertainties add in the root mean square (RMS) sense:

$$\Delta S^{ran}\left(\mathbf{x_0}\right)=\sqrt{\sum_{i=1}^{M}\left[\frac{\partial S}{\partial x_i}\left(\mathbf{x_0}\right)\cdot\Delta x_i^{ran}\left(\mathbf{x_0}\right)\right]^2} \tag{4}$$

The vector $\mathbf{x_0}$ stands for the set of unperturbed parameters $x_{i0}, i=1,\ldots M$.

2) The conservative method for the propagation of systematic errors would be to added them up in an absolute sense:

$$\Delta S^{sys}\left(\mathbf{x_0}\right)=\sum_{i=1}^{M}\left|\frac{\partial S}{\partial x_i}\left(\mathbf{x_0}\right)\cdot\Delta x_i^{sys}\left(\mathbf{x_0}\right)\right| \tag{5}$$

However, frequently, the rule for adding random errors (equation(4)) is also used for the propagation of systematic errors. This is based on the assumption that the various systematic errors have different signs and thus cancellation can occur in a similar ways as for random errors. For the Aquarius L2 error computation we have adopted this philosophy when computing systematic errors.

2.3 Uncertainty Propagation in L3 Averaging

Assuming we have $j=1,\ldots N$ L2 salinity retrievals S_j at a certain cell with individual random errors ΔS_j^{ran}, individual systematic errors ΔS_j^{sys} and individual total RMS error $\Delta S_j=\sqrt{\left(\Delta S_j^{sys}\right)^2+\left(\Delta S_j^{ran}\right)^2}$. The L3 product can be formed as weighted average:

$$\bar{S} \quad =\frac{\sum_{j=1}^{N}\left[w_j\cdot S_j\right]}{\sum_{j=1}^{N}w_j} \tag{6}$$

with weights $w_j, j=1,\ldots N$ and $w_j>0$. The standard weighting is to set $w_j=1$ for all j, which is adopted in Aquarius V4.0. An optimum weighting scheme that minimizes the total RMS uncertainty of the average would be to choose $w_j=\frac{1}{\left(\Delta S_j\right)^2}$ (0).

The following rules apply for calculating the systematic error ΔS^{sys} and the random error ΔS^{ran} of the L3 product in V4.0:

1. The systematic uncertainty of the L3 product is computed as:

$$\Delta \bar{S}^{sys} = \frac{1}{\sum_{j=1}^{N} w_j} \cdot \sum_{j=1}^{N} \left[w_j \cdot \left| \Delta S_j^{sys} \right| \right] \tag{7}$$

That means that when going from L2 to L3 we apply the conservative method (5) for propagation of systematic errors and do not allow error cancellation.

2. The random uncertainty (standard deviation) of the weighted L3 average is computed as:

$$\Delta \bar{S}^{ran} = \frac{1}{\left[\sum_{j=1}^{N} w_k \right]} \cdot \sqrt{\sum_{k=1}^{N} \left[w_k \cdot \left(\Delta S_k^{ran} \right) \right]^2} \tag{8}$$

Equation (8) follows from calculating the *standard deviation of the mean*:

$$\Delta \bar{S}^{ran} = \sigma\left(\bar{S}\right) = \sqrt{\sum_{k=1}^{N} \left[\frac{\partial \bar{S}}{\partial S_k} \cdot \left(\Delta S_k^{ran} \right) \right]^2} \tag{9}$$

and inserting the expression (6). For the special case of equal random errors $\Delta S_i^{ran} = \Delta S^{ran},\ i = 1 \ldots N$ and equal weighting $w_i = 1, i = 1, \ldots N$ equation (8) reduces to the familiar $1/\sqrt{N}$ suppression rule for the random error in averages:

$$\Delta \bar{S}^{ran} = \frac{\Delta S^{ran}}{\sqrt{N}} \tag{10}$$

3. ERROR MODEL

This section discusses the major error sources of the Aquarius salinity retrieval algorithm and the quantitative assessment of their uncertainty.

3.1 NEDT

The radiometer noise (NEDT) is computed as the standard deviation of the RFI filtered antenna temperatures (TF) computed over each 1.44 second cycle. Because the L2 salinity is retrieved at each 1.44 sec cycle, this noise figure needs to be divided by the number of valid observations within that cycle that are used in the computation of the cycle average of TF. This error is treated as random error. We compute the NEDT and the resulting error in the salinity for all 3 channels in TF: V-pol, H-pol and the 3rd Stokes. These 3 components are independent and therefore the resulting errors in the salinity can be added as root sum squares.

3.2 Sensor Pointing Errors

In order to estimate the magnitude of the sensor pointing knowledge error we compute the difference between nominal pointing (nadir) and the actual pointing that is computed from the measured S/C attitude. This value is the combination of both pointing knowledge error and pointing control error and it thus can be regarded as an upper limit for the pointing knowledge error [Patt, 2015]. It is impossible to make separate assessments of knowledge and control errors. The pointing error is treated as a random error. It turns out that its size and contribution to the total uncertainty is less than 0.01 psu and thus negligible.

3.3 Surface Wind Speed and Direction

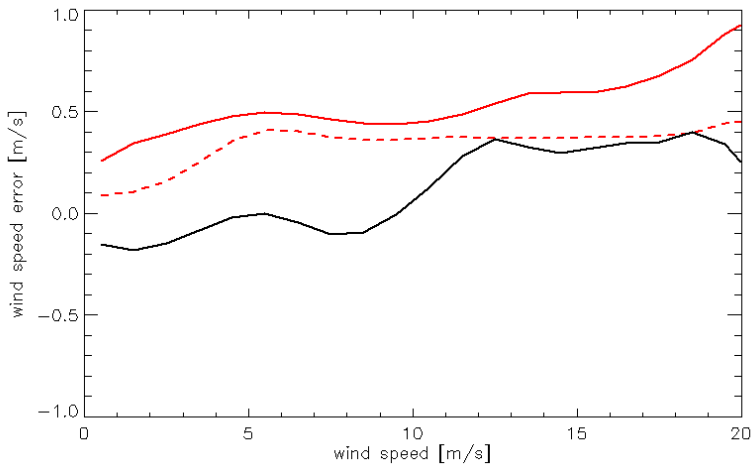

Figure 1: Estimated error of surface wind speed that is used in the Aquarius SSS retrieval: Dashed red line: Estimated random error from perturbed HHH wind speed retrieval. This curve is used as error model in the uncertainty estima-

tion of the SSS retrievals. Full red line: random difference between Aquarius HHH and WindSat wind speed divided by $\sqrt{2}$. Black line: Estimated systematic error from Aquarius HHH – WindSat comparison.

The estimated random component (dashed red line in Figure 1) is based on running perturbed Aquarius HHH wind speed retrievals [Meissner et al., 2014a]. The major error sources are the noise in the radiometer observations (NEDT) and the scatterometer observations (Kp-value) observations and errors in the auxiliary NCEP wind speed that is used as background field.

The full red line in Figure 1 depicts the standard deviation of the difference between the Aquarius HHH wind speed and collocated WindSat wind speed [Meissner et al., 2014a] after dividing by $\sqrt{2}$. The division by $\sqrt{2}$ accounts for the fact that part $(1/2)$ of the observed random difference comes from errors in the Aquarius wind speeds and the other part $(1/2)$ comes from errors in the WindSat wind speed. This assumption is supported by a triple point analysis of Aquarius, WindSat and buoy wind speeds [Meissner et al., 2014a]. We have checked that using the full red line as model for the random error ΔW^{ran} in wind speed in the uncertainty analysis would result in uncertainty estimates for the Aquarius salinities that are too large when comparing with ground truth observations (c.f. section 4.4). This applies in particular at high wind speeds. As explained above, the dashed line from Figure 1 is computed as the formal estimate for the error ΔW^{ran} in the Aquarius HHH wind speed and it turns out that using it instead of the full red line results in a more realistic uncertainty estimate for the retrieved Aquarius salinity. The conclusion is that the random error estimate in the Aquarius HHH wind speed estimate from the ground truth comparison (full red line in Figure 1) is too large, in particular at high . A possible explanation is that sampling mismatch between Aquarius and WindSat observation might also contribute to the observed value of the standard deviation. This sampling mismatch error is expected to increase with wind speed.

The estimate of the systematic component ΔW^{sys} of this error is computed as the bias between Aquarius HHH and WindSat wind speed as function of wind speed (black line in Figure 1). As was the case for the random error in the Aquarius HHH wind speed it can also be assumed that part of the observed systematic error is due to the WindSat wind speed. One should regard the systematic uncertainty ΔW^{sys} in the Aquarius HHH wind speed obtained from the full black curve in Figure 1 as an upper limit for the systematic uncertainty in the Aquarius HHH wind speeds.

The error in the auxiliary NCEP wind direction φ is assumed to be a random error and we assume a value of $\Delta\varphi=10^{o}$.

3.4 Auxiliary SST Input

The estimated uncertainty ΔSST in the auxiliary SST input is treated as systematic error. It is computed at each Aquarius L2 observation by comparing the NOAA OI SST that is used in the Aquarius V4.0 SSS retrievals with weekly 0.25^{o} SST average maps from WindSat, which are space-time interpolated to the Aquarius observation.

Figure 2 shows the monthly difference between Reynolds and WindSat SST.

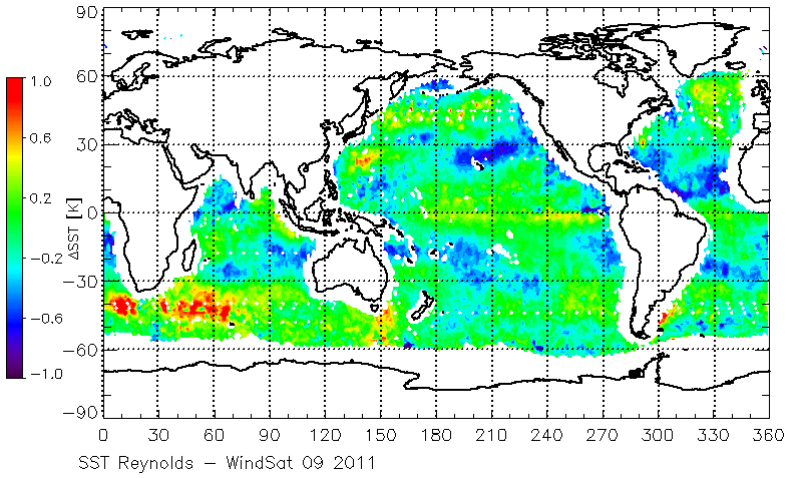

Figure 2: SST difference between SST from Reynolds and WindSat for September 2011.

3.5 Non-Linear IU Coupling

The comparison between T_B measured by Aquarius (T_{Bmeas}) and expected (T_{Bexp}), which is calculated from the geophysical model function using the HYCOM SSS field as input, reveals a significant non-linear crosstalk between 1st Stokes parameter I and 3rd Stokes parameter U (Figure 3). Because the crosstalk is non-linear, it cannot be corrected explained by an error in the antenna patter correction (APC), which transforms antenna temperatures (T_A) into brightness temperatures (T_B) [Wentz et al., 2012]. Aquarius V4.0 applies an empirical correction for this observed non-linear IU coupling [Wentz et al., 2015]. We have included the size of the coupling (Figure 3) as systematic error into the uncertainty estimate.

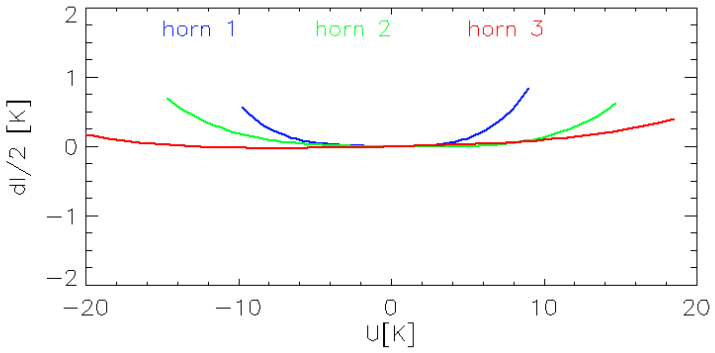

Figure 3: Estimated error in the Aquarius 1st Stokes parameter I/2 = (T_{BV} + T_{BH})/2 through coupling from the 3rd Stokes parameter U. The curves displayed in the figure are obtained from polynomial fits to the data for each of the three Aquarius horns.

3.6 Reflected Galactic and Lunar Radiation

The estimated uncertainty in the correction for the reflected galactic radiation is treated as systematic error and its computation is based on a 2-dimensional stratification of the bias T_{Ameas} – T_{Aexp} versus the $T_{Agal,ref}$ of I/2 and the Aquarius wind speed (Figure 4). The values in Figure 4 characterize the degradation of the salinity retrievals [Meissner, 2014b]. T_{Aexp} is obtained using the HYCOM SSS as surface truth for salinity.

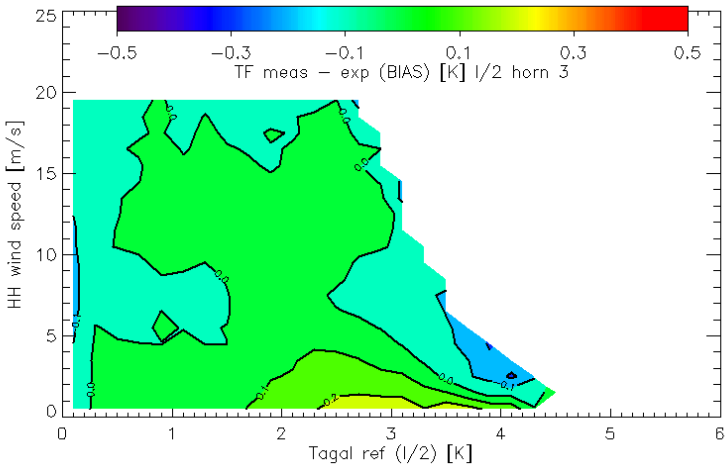

Figure 4: Bias of T_{Ameas} – T_{Aexp} stratified as function of reflected galactic radiation and Aquarius HH wind speed. The curves have been computed from 3 years of data SEP 2011 – AUG 2014.

The uncertainty for the reflected lunar radiation is based on stratifying $T_{Ameas} - T_{Aexp}$ versus $T_{Amoon,ref}$ (Figure 5). The lunar correction does not use wind speed as it assumes a specular surface. Therefore the stratification in Figure 5 does not include wind speed as parameter either.

In the uncertainty estimate we use Figure 4 and Figure 5 as lookup tables in order to estimate the systematic uncertainties $\Delta T_{AI,gal,ref}/2 = (\Delta T_{AV,gal,ref}+\Delta T_{AH,gal,ref})/2$, i.e. the average of V-pol and H-pol TA.

Figure 4 and Figure 5 depict the values for the biases of $T_{Ameas} - T_{Aexp}$ as function of the reflected galaxy and lunar radiation. The corresponding plots for the standard deviations give small values compared with the bias values. We therefore use only the biases for the uncertainty estimates.

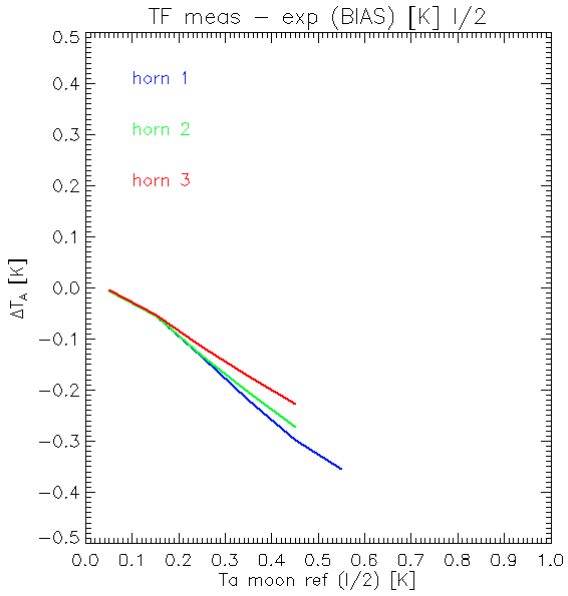

Figure 5: Bias of $T_{Ameas} - T_{Aexp}$ stratified as function of reflected moon radiation. The curves have been computed from 3 years of data SEP 2011 – AUG 2014.

It is assumed that the galactic radiation itself is unpolarized and polarization occurs only through the reflection at the ocean surface. The uncertainty in the 2nd Stokes parameter $\Delta T_{AQ,gal,ref} = \Delta T_{AV,gal,ref} - \Delta T_{AH,gal,ref}$ of the reflected galactic radiation can then be approximately calculated from equation (14) in [Wentz et al., 2014] based on the reflectivity ratio:

$$\Delta T_{AQ,gal,ref} \approx \frac{R_V - R_H}{R_V + R_H} \cdot \Delta T_{AI,gal,ref} \approx \frac{T_{AQ,gal,ref}}{T_{AI,gal,ref}} \cdot \Delta T_{AI,gal,ref} \qquad (11)$$

That means the uncertainties in the 1st and the 2nd Stokes parameters of the reflected galactic radiation are correlated. As a consequence the uncertainties in the V-pol and H-pol TA of the reflected galaxy are correlated as well. The situation is different than in the case of the NEDT (section Sensor Pointing Errors3.1), where the uncertainties in V-pol and H-pol TA are uncorrelated. When performing the perturbed retrievals, it is important to treat these channel correlations properly. As in equation (14) of [Wentz et al., 2014] we set the uncertainty in the 3rd Stokes parameter of the galactic radiation to zero. The same rules apply when estimating the uncertainty in the reflected lunar radiation.

3.7 Intruding Radiation from Land and Sea Ice

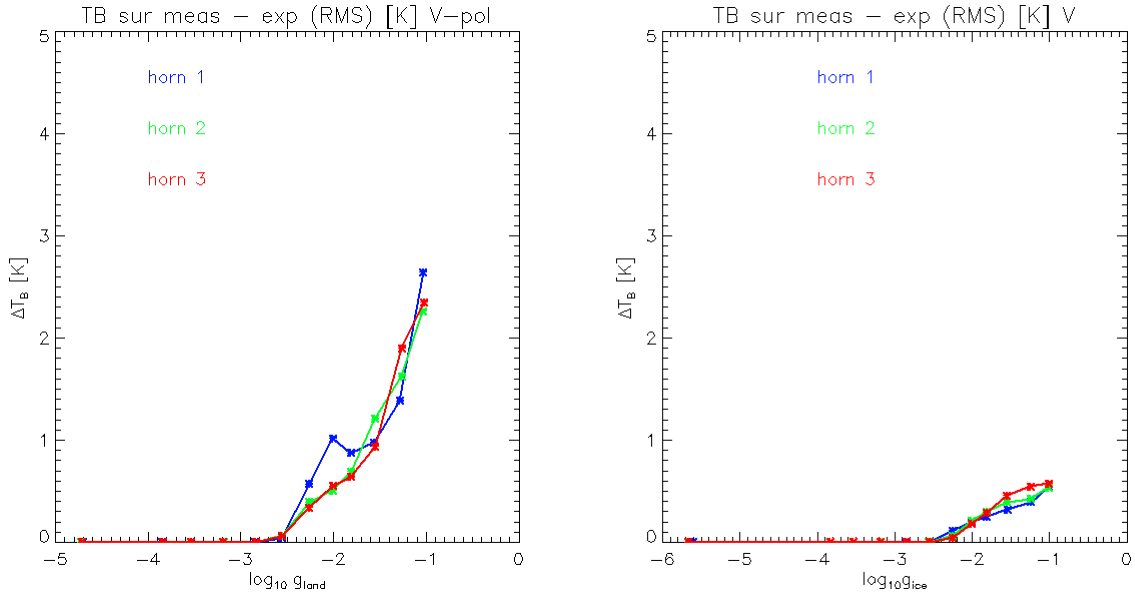

Figure 6: RMS of $T_{Bmeas} - T_{Bexp}$ for the V-pol stratified as function of the gain weighted land fraction g_{land} (left) and gain weighted sea ice fraction g_{ice} (right). The curves have been computed from 3 years of data SEP 2011 – AUG 2014.

The estimated uncertainty due to intrusion of radiation from land and sea ice surfaces into the sidelobes of the Aquarius antenna is treated as systematic and based on computing the RMS of $T_{Bmeas} - T_{Bexp}$ and stratifying it versus the gain weighted fractions of land g_{land} and sea ice g_{ice} within the Aquarius antenna footprint (Figure 6). The RMS of $T_{Bmeas} - T_{Bexp}$ is the root sum square of bias and standard deviation and both of them give a significant contribution to the whole RMS. As was the case for the reflected galaxy and lunar radiation, the uncertainty estimates for the intrusions from land and sea ice are based on studying the degradation of the retrieval algorithm by

comparing with ground truth observations, in this case the HYCOM SSS [Meissner, 2014b]. When computing the variance $\sigma^2(T_{Bmeas} - T_{Bexp})$ as function of g_{land} and g_{ice} we have subtracted the *noise floor*, which is the value for $\sigma^2(T_{Bmeas} - T_{Bexp})$ over the open ocean. i.e. if g_{land}=0 and g_{ice}=0, because we consider only the uncertainty in $T_{Bmeas} - T_{Bexp}$ that arises from the degradation due to intruding radiation from land and sea ice surfaces. Curves as shown in Figure 6 are produced for all three horns and for both V-pol and H-pol $T_{Bmeas} - T_{Bexp}$. When running the perturbed retrievals we look up the values for $T_{Bmeas} - T_{Bexp}$ in all of the channels based on the actual values of g_{land} and g_{ice}. As was the case in section 3.6, this results in correlated uncertainties for V-pol and H-pol T_B for each horn.

3.8 Undetected RFI

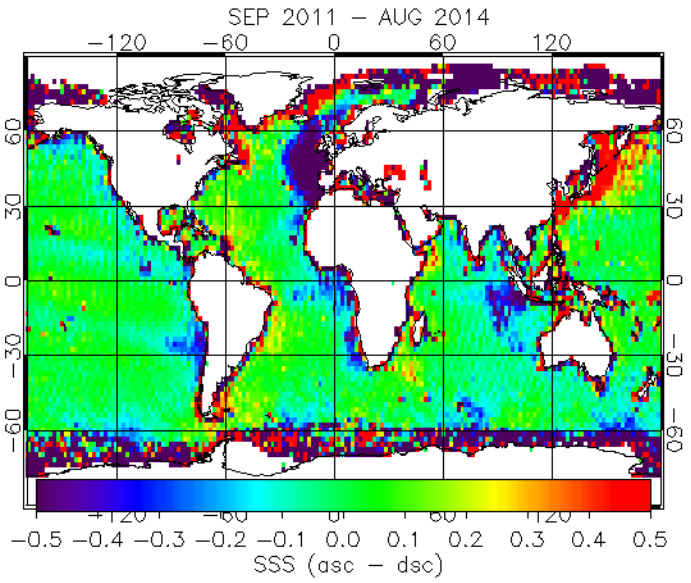

Figure 7: Map of the salinity difference between ascending and descending Aquarius swaths for SEP 2011 – AUG 2014.

The uncertainty from undetected RFI can be estimated from the SSS differences between ascending and descending Aquarius swaths [Meissner, 2014b]. It is treated as systematic uncertainty. For the formal uncertainty estimate we first create a static 3-year map of the difference between ascending (PM) and descending (AM) Aquarius SSS summing over all three horns (Figure 7). The next step is to create a mask of areas where undetected RFI is likely present. As discussed in [Meissner, 2014b], this can be done by creating peak hold maps of RFI filtered – unfiltered TA sep-

arate for ascending and descending swaths, mask cells where this difference exceeds a threshold (0.2 K) and then extend this mask by a certain amount (+/- 4^{o}) in order to account for the fact that the undetected RFI can enter through the antenna sidelobes.

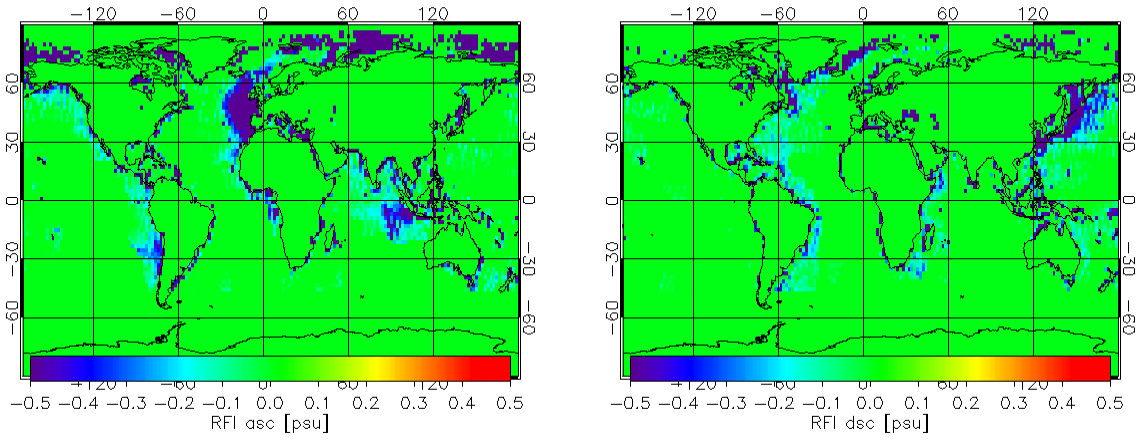

Figure 8: Estimated uncertainty in the retrieved Aquarius salinity due to undetected RFI for the ascending swath (left) and the descending swath (right) after averaging over all 3 horns.

Because undetected RFI always results in low salinity value, we can create maps of the estimated salinity uncertainties from undetected RFI for the ascending swaths if $SSS_{asc} - SSS_{dsc} < 0$ and for the descending swaths if $SSS_{asc} - SSS_{dsc} > 0$ and if the cells falls within the extended masks. This results in the two maps of Figure 8. Unlike all other uncertainties, the uncertainty estimate due to uncertainty RFI is done directly on the salinity level. The uncertainty maps are static, i.e. we assume the same values for the whole Aquarius mission and we are averaging over all three horns, i.e. the uncertainties are not horn specific.

3.9 Uncertainties that are Not Considered or Neglected

Our error model does not consider or access the uncertainties listed in

Table 1, because they are either estimated to be negligible or because it is not possible to make a realistic assessment of their sizes.

Table 1: Error sources that are not considered or neglected in the uncertainty estimate.

Error Source	Reason for not considering
Atmospheric temperature	Estimated to be small. The estimated sensitivity of the retrieved salinity to the average value of the atmospheric temperature is less than 0.05 psu/K. Assuming similar uncertainties in the values of the ancillary atmospheric temperatures as the ones in the ancillary SST (Figure 2) will result in small or negligible errors in the retrieved salinity.
Atmospheric vapor	Very small signal and therefore very small uncertainty.
Atmospheric liquid cloud water	Difficult to estimate as long as ancillary NCEP liquid cloud water profiles are used in the retrieval algorithm. When comparing with cloud water values from microwave radiometer (SSMIS, WindSat) or CMORPH, the cloud water values from NCEP are statistically compatibly with zero. Calculating the cloud water absorption from the ancillary NCEP liquid cloud water profile is merely a placeholder in the V4.0 algorithm. It is necessary and planned in the future to use a realistic ancillary field (e.g. CMORPH) for computing the liquid cloud water absorption.
Solar intrusion (direct, reflected, backscattered)	Very small signal and therefore very small uncertainty.
Direct galaxy + cold space	Difficult to estimate.
Instrument calibration	We assume perfect absolute calibration to the RTM. We assume that all residual biases have been corrected in the updated RTM [Wentz et al., 2015].
APC coefficients	
RTM	

4. RESULTS

4.1 Error Allocations at L2 and L3

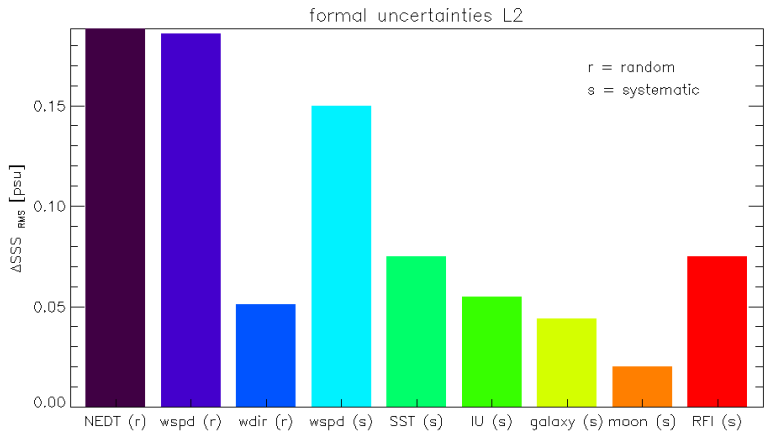

Figure 9: Contribution of the various uncertainties to the total estimated uncertainty for the Aquarius L2 salinity that is observed at the 1.44 sec cycle for open ocean scenes.

Figure 9 and Figure 10 show the contributions of the various components of the error model (section 3) to the total formal uncertainty estimate for the Aquarius L2 product (1.44 sec) and the monthly 1° L3 salinity products respectively. The dominant contributions at the 1.44 sec are the NEDT and the random and systematic uncertainties in the wind speed that is used in the surface roughness correction algorithm. At the monthly 1° Level 3 product all the random uncertainties including the NEDT get reduced to low levels.

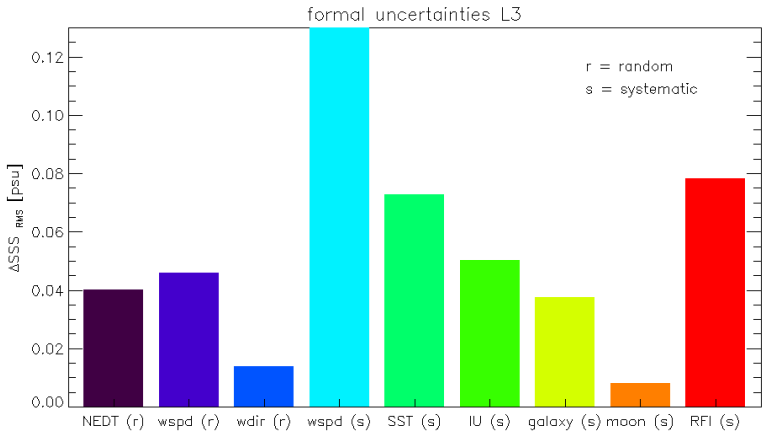

Figure 10: Contribution of the various uncertainties to the total estimated uncertainty for the monthly 1° Aquarius L3 salinity maps for open ocean scenes.

4.2 Time Series

Figure 11 shows a monthly time series of the estimated RMS uncertainty in the L2 Aquarius salinity compared with the RMS of the difference between Aquarius and HYCOM salinity. As expected, the formal error estimate comes in somewhat lower than the comparison with HYCOM, because part of the difference between Aquarius and HYCOM is caused by the fact that the HYCOM model salinity field does not fully represent the satellite salinity measurement due to temporal and spatial mismatch and there are also errors in the HYCOM field itself.

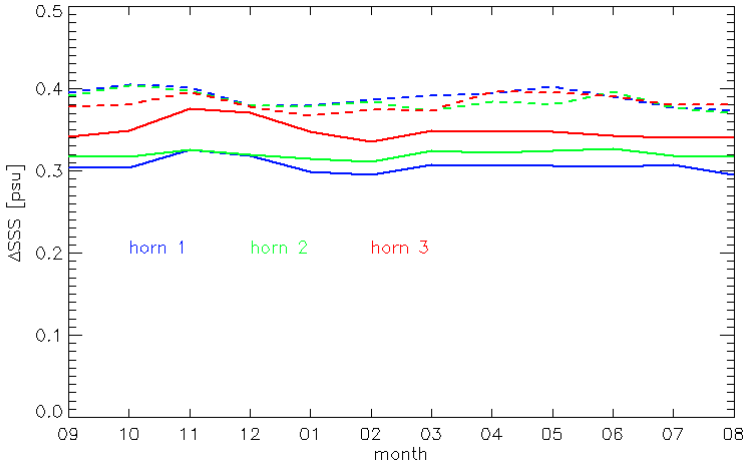

Figure 11: Monthly time series of the RMS for the total estimated uncertainty in the Aquarius L2 product for SEP 2011 – AUG 2012. The full lines are the formal uncertainty estimates for the 3 horns. The dashed lines are the RMS of the difference between Aquarius and HYCOM salinity.

4.3 Global Maps

Figure 12 shows a global map of the total estimated RMS of a monthly L3 salinity. As expected, the uncertainty increases in cold SST due to diminishing sensitivity and it also increases close to land and sea ice.

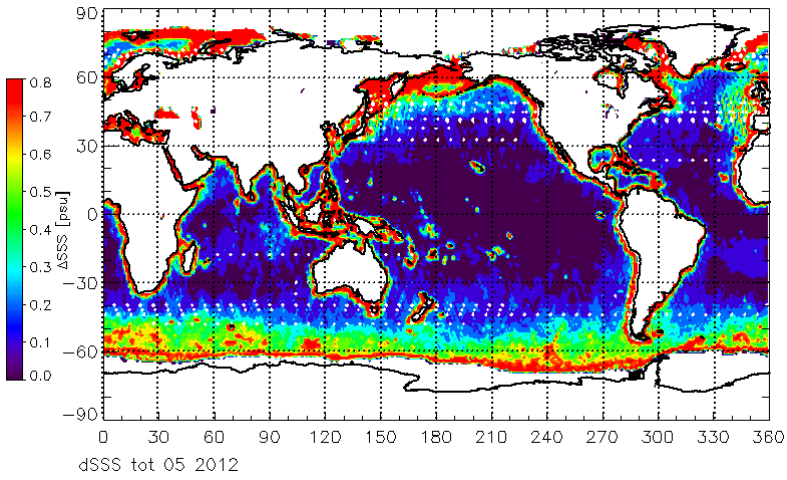

Figure 12: Total estimated RMS uncertainty of the monthly 1° Aquarius L3 salinity map for May 2012.

4.4 Formal Error Estimate versus Comparison with Ground-Truth Validation Sources

In order to judge how realistic the formal uncertainty estimates are it is instructive to compare them with uncertainty estimates that can be obtained from comparing Aquarius salinity measurements with *ground truth* observations. The method that is also used for validating the Aquarius accuracy mission requirement uses a triple collocation analysis of salinity values that were measured by Aquarius, HYCOM and ARGO drifters. Our triple collocation set uses ARGO data taken from the monthly 3-deg gridded ADPRC field provided by the University of Hawaii (apdrc.soest.hawaii.edu). Assuming that the errors in the three salinity measurements (Aquarius, HYCOM, ARGO) are mutually independent, the laws of error propagation allow assessing the mean square error (variance) of each of the salinity measurements from the mean square of the mutual differences. For example, the mean square error in the Aquarius (Aq) salinity measurement is given by:

$$\mathrm{Var}(\mathrm{Aq}) = \frac{1}{2}\left[\mathrm{Var}(\mathrm{Aq}\text{ - }\mathrm{HYCOM}) + \mathrm{Var}(\mathrm{Aq}\text{ - }\mathrm{ARGO}) - \mathrm{Var}(\mathrm{HYCOM}\text{ - }\mathrm{ARGO})\right] \quad (12)$$

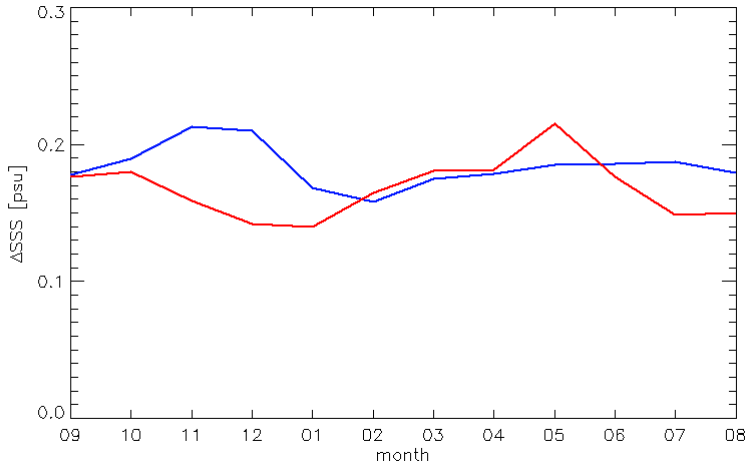

Figure 13: Time series of monthly 3º Aquarius L3 uncertainties SEP 2011 – AUG 2012: Blue =RMS of formal estimate. Red= RMS of estimate from triple collocation analysis.

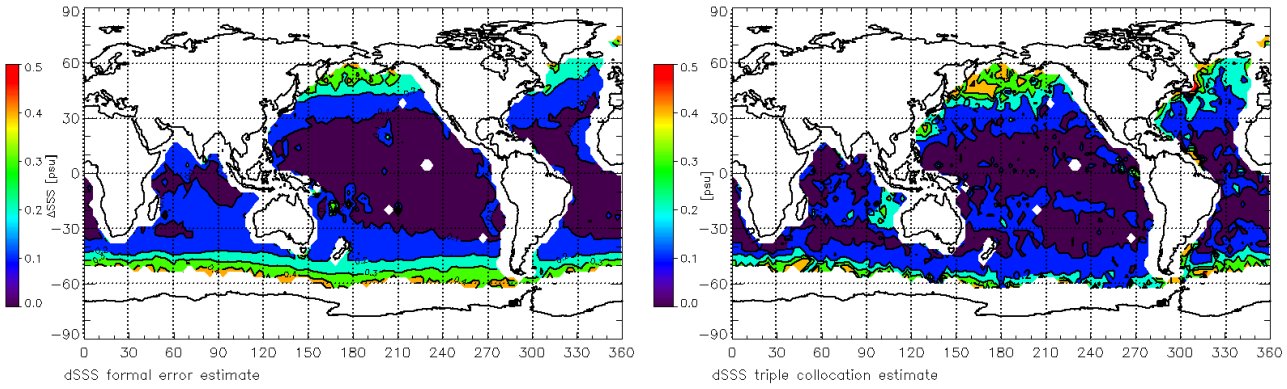

Figure 14: Estimated RMS error of Aquarius salinity the open ocean: Left: From formal .uncertainty. Right: From triple collocation analysis.

This triple collocation analysis can be applied to a time series of monthly maps of salinity differences between Aquarius, HYCOM and ARGO, which results in a time series of monthly uncertainty estimates of the Aquarius salinity. This is the red curve in Figure 13.

The triple collocation analysis can be applied to a map of time series of monthly salinity differences between Aquarius, HYCOM and ARGO, which results in a map of estimates of the Aquarius salinity uncertainty. This is the right map in Figure 14. In both instances it is possible to compare directly with the results of the formal uncertainty estimate, which are the blue curve in Figure 13 and the left map of Figure 14. In both cases there is very good agreement between the formal uncertainty estimate and the uncertainty obtained from the triple collocation method.

5. IMPLEMENTATION IN VERSION 4.0

The perturbed V4.0 L2 Aquarius salinity retrievals were run at Remote Sensing Systems for the time period SEP 2011 – AUG 2012 and from that a monthly 1^{o} climatology of L3 uncertainty maps was created. The L3 uncertainties were separated into random and systematic and separate L3 uncertainty maps were created for the ascending (PM) and descending Aquarius swaths. Rather than running the perturbed retrievals at ADPS we have created monthly climatology maps of L2 uncertainties from the L3 maps using the following prescription:

$$\begin{aligned} \sigma_{sys}^{L2} &= \sigma_{sys}^{L3} \\ \sigma_{ran}^{L2} &= \sqrt{N} \cdot \sigma_{ran}^{L3} \end{aligned} \tag{13}$$

where N is the monthly population of each grid cell. When running the L2 processor at ADPS, the

L2 climatology uncertainty map is interpolated in space and time to the Aquarius observation. The obtained L2 uncertainty estimate can be regarded as an estimate for a typical uncertainty rather than the actual uncertainty form the perturbed retrieval.

For future data releases it is planned to calculate an uncertainty for each salinity retrieval by running a full perturbed salinity algorithm for each L2 observation at ADPS.

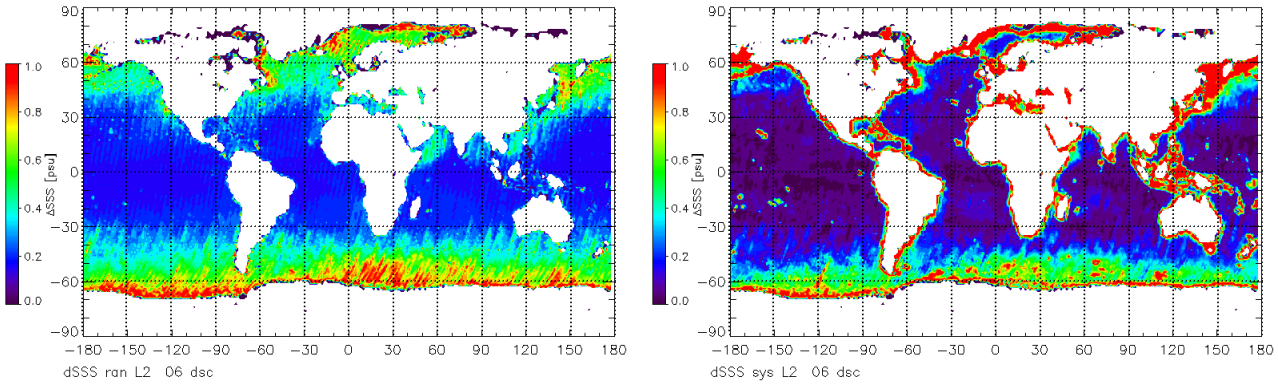

Figure 15: Climatology of Level 2 Aquarius salinity uncertainties obtained from equation (13) for the month of June. Left = random uncertainty. Right = systematic uncertainty. This estimate of a typical L2 uncertainty is used in the ADPS V4.0 data release.

6. REFERENCES

Meissner, T., F. Wentz and L. Ricciardulli, The emission and scattering of L-band microwave radiation from rough ocean surfaces and wind speed measurements from the Aquarius sensor, JGR Oceans, vol. 119, doi: 10.1002/2014JC009837, 2014a.

Meissner, T., Performance degradation and Q/C flagging of Aquarius L2 salinity retrievals, report number 031814, Remote Sensing Systems, Santa Rosa, CA, 2014b.

Patt, F., GSFC, private communication, 2015.

Wentz, F. et al., Aquarius salinity retrieval algorithm, Algorithm Theoretical Basis Document, Version 2 (2012), Addendum I (2012), Addendum II (2013), Addendum III (2014), Addendum IV (2015), http://podaac.jpl.nasa.gov/SeaSurfaceSalinity/Aquarius.

APPENDIX A. OPTIMUM WEIGHTING FOR LEVEL 3 AVERAGING

An optimum weighting for creating a best estimate S_{est} from individual measurements $S_j, j = 1,\ldots N$ can be derived as follows:

Given S_j realizations of random variable that is Gaussian distributed around S_{est} with individual uncertainties are ΔS_j^{ran}, the probability that the measurement j gives a value S_j is proportional to:

$$P\left(S_j\right) \propto \frac{1}{\Delta S_j^{ran}} \cdot \exp\left[-\frac{\left(S_j - S_{est}\right)^2}{2 \cdot \left(\Delta S_j^{ran}\right)^2}\right] \tag{14}$$

Because the realizations are independent the probability to obtain the joint realization $S_1, S_2, \ldots S_N$ is the product of the individual terms in (14) and thus:

$$P\left(S_1, S_2, \ldots S_N\right) \propto \frac{1}{\left(\Delta S_1^{ran}\right) \cdot \ldots \cdot \left(\Delta S_N^{ran}\right)} \cdot \exp\left[-\sum_{j=1}^{N} \frac{\left(S_j - S_{est}\right)^2}{2 \cdot \left(\Delta S_j^{ran}\right)^2}\right] \tag{15}$$

The best estimate S_{est} is obtained if this probability has a maximum, which means that the negative exponent in (15) itself has a minimum:

$$\chi^2\left(S_{est}\right) = \sum_{j=1}^{N} \frac{\left(S_j - S_{est}\right)^2}{\left(\Delta S_j^{ran}\right)^2} \tag{16}$$

Differentiating (16) with respect to S_{est} gives:

$$\frac{\partial \chi^2\left(S_{est}\right)}{\partial S_{est}} = 2 \cdot \sum_{j=1}^{N} \frac{\left(S_j - S_{est}\right)}{\left(\Delta S_j^{ran}\right)^2} = 2 \cdot \sum_{j=1}^{N} \frac{S_j}{\left(\Delta S_j^{ran}\right)^2} - 2 \cdot S_{est} \cdot \sum_{j=1}^{N} \frac{1}{\left(\Delta S_j^{ran}\right)^2} \tag{17}$$

Solving (17) for S_{est} gives:

$$S_{est} = \frac{1}{\sum_{j=1}^{N} \frac{1}{\left(\Delta S_j^{ran}\right)^2}} \cdot \sum_{j=1}^{N} \frac{S_j}{\left(\Delta S_j^{ran}\right)^2} \tag{18}$$

This is equation (6) with $w_j = \frac{1}{\left(\Delta S_j^{ran}\right)^2}$.

More generally, one could substitute the random component ΔS_j^{ran} by the total RMS error $\Delta S_j = \sqrt{\left(\Delta S_j^{sys}\right)^2 + \left(\Delta S_j^{ran}\right)^2}$, which means $w_j = \frac{1}{\left(\Delta S_j\right)^2}$.